Journal of Solid Mechanics Vol. 5, No. 1 (2013) pp. 74-91

Axi-Symmetric Deformation Due to Various Sources in Saturated Porous Media with Incompressible Fluid

R. Kumar[1,*], S. Kumar[2], M.G. Gourla[3]

[1]*Department of Mathematics, Kurukshetra University, Kurukshetra, Haryana, India*
[2]*Department of Mathematics, Govt. Degree College Indora (Kangra), Himachal Pradesh, India*
[3]*Department of Mathematics, Himachal Pradesh University, Shimla-171005, India*

Received 19 February 2013; accepted 8 April 2013

ABSTRACT

The general solution of equations of saturated porous media with incompressible fluid for two dimensional axi-symmetric problem is obtained in the transformed domain. The Laplace and Hankel transforms have been used to investigate the problem. As an application of the approach concentrated source and source over circular region have been taken to show the utility of the approach. The transformed components of displacement, stress and pore pressure are obtained. Numerical inversion technique is used to obtain the resulting quantities in physical domain. Effect of porosity is shown on the resulting quantities. A particular case of interest is also deduced from the present investigation.

Keywords: Axi-symmetric; Incompressible porous medium; Pore pressure; Laplace transform; Hankel transform; Concentrated source and source over circular region

1 INTRODUCTION

THE dynamic response due to various sources in a saturated porous media with incompressible fluid are of great interest in geophysics, acoustic, soil and rock mechanics and many earthquake engineering problems.

Biot [1] derived the basic equations of poroelastisity on the basis of energy principles. Privost [2] rederived these equations by use of mixture theory. Zienkiewicz, Chang and Bettess [3], Zienkiewicz and Shiomi [4] derived the basic equations of poroelasticity by the use of principal of continuum mechanics. Gatmiri and Kamalian [5] adopted the later approach because it is more flexible and is based on a set of parameters with a clear physical interpretation to discuss different type of problem. Gatmiri and Nguyen [6] investigated two dimensional problem for saturated porous media with incompressible fluid. Gatmiri and Jabbari [7, 8] discuss time domain Green'_s functions for unsaturated soil for two dimensional and three dimensional solution. Gatmiri, Maghoul and Duhamel [9] also discuss the two dimensional transient thermo-hydro-mechanical fundamental solution of multiphase porous media in frequency and time domains. Gatmiri and Eslami [10] discuss the scattering of harmonic waves by a circular cavity in a porous medium by using complex function theory approach. Kumar, Singh and Chadha [11] discuss axisymmetric problem in microstrecth elastic solid. Kumar and Singh [12] also discuss elastodynamics of an axisymmetric problem in microstrecth viscoelastic solid. Kaushal, Kumar and Miglani [13] discuss the response of frequency domain in generalized thermoelasticity with two temperature. Kumar, Garg and Miglani [14] also discuss elastodynamics of an axisymmetric problem in an anisotropic liquid-saturated porous medium.

Oliveira, Dumont, Selvadura [15] discuss boundary element formulation of axisymmetric problems for an elastic half space. The influence of the finite initial strains on the axisymmetric wave dispersion in a circular cylinder

* Corresponding author.
E-mail address: rajneesh_kuk@rediffmail.com (R.Kumar).

embedded in a compressible elastic medium has been discussed by Akbarov and Guliev [16].Gordeliy, Detourna [17] investigated the displacement discontinuity method for modelling axisymmetric cracks in an elastic half-space.

In the present paper, we obtain the components of displacement, stress and pore pressure due to concentrated source and source over circular region in the time domain and frequency domain in saturated porous media with incompressible fluid. The resulting quantities are shown graphically to depict the effect of porosity.

2 GOVERNING EQUATIONS

Following Gatmiri and Nugyen [6], the basic equations are

Equation of motion:

$$\sigma_{ij,j} + f_i = \rho \ddot{u}_i + \rho_f \ddot{w}_i \tag{1}$$

Constitutive relation:

$$\sigma_{ij} = \lambda u_{k,k}\delta_{ij} + \mu(u_{i,j} + u_{j,i}) - \alpha p \delta_{ij} \tag{2}$$

Flow conservation for the fluid phase:

$$-\dot{w}_{i,i} + \gamma = \alpha \dot{u}_{k,k} + \frac{\dot{p}}{M} \tag{3}$$

Generalized Darcy's law:

$$p_{,i} = -\frac{1}{\kappa}\dot{w}_i - \rho_f \ddot{u}_i - m\ddot{w}_i \tag{4}$$

where u_i is the displacement of the solid skeleton, p denote the fluid pressure, w_i represents the average displacement of the fluid relative to the solid. The elastic constants λ and μ are drained Lame's constant. ρ_f is the fluid density, ρ_s is the solid density, $\rho = (1-n)\rho_s + n\rho_f$ is the density of solid-fluid mixture and $m = \frac{\rho_f}{n}$ is the mass parameter where n is the porosity, κ is the permeability coefficient. α and M are material parameters which describes the relative compressibility of the constituents. f_i and γ denotes the body force and the rate of fluid injection into the media.

Eqs. (1) and (4) with the aid of (2) and (3) in the absence of body force and the rate of fluid injection into the media ,reduce to:

$$\mu u_{i,jj} + (\lambda + \mu)u_{k,ki} - \rho_1 \ddot{u}_i - \alpha^* p_{,i} = 0 \tag{5}$$

$$\tau p_{,ii} - \frac{1}{M}\frac{\partial p}{\partial t} - \alpha^* \dot{u}_{k,k} = 0 \tag{6}$$

where

$$\rho_1 = \rho - \rho_f^2 \tau \frac{\partial}{\partial t}, \alpha^* = \alpha - \rho_f \tau \frac{\partial}{\partial t}, \tau = \left[\frac{1}{\kappa} + m\frac{\partial}{\partial t}\right]^{-1}$$

3 FORMULATION OF THE PROBLEM

We consider a saturated porous media with incompressible fluid whose boundaries are parallel to the plane z=0 in the cylindrical polar coordinate system (r,θ,Z). We consider a two-dimensional axi-symmetric problem with symmetry about z-axis, so that all the quantities are remained independent of θ and $\frac{\partial}{\partial\theta}=0$ .The complete geometry of the problem is shown in the Fig. 1(a),1(b). We assume the components of displacement vector as:

$$\vec{u}=(u_r,0,u_z) \tag{7}$$

Eqs. (5) and (6) with the aid of (7) can be written as:

$$\mu(\nabla^2-\frac{1}{r^2})u_r+(\lambda+\mu)\frac{\partial e}{\partial r}-\alpha^*\frac{\partial p}{\partial r}=\rho_1\frac{\partial^2 u_r}{\partial t^2} \tag{8}$$

$$\mu\nabla^2 u_z+(\lambda+\mu)\frac{\partial e}{\partial z}-\alpha^*\frac{\partial p}{\partial z}=\rho_1\frac{\partial^2 u_z}{\partial t^2} \tag{9}$$

$$\tau\nabla^2 p-\alpha^*\frac{\partial e}{\partial t}-\frac{1}{M}\frac{\partial p}{\partial t}=0 \tag{10}$$

where

$$e=\frac{\partial u_r}{\partial r}+\frac{1}{r}u_r+\frac{\partial u_z}{\partial z},\nabla^2=\frac{\partial^2}{\partial r^2}+\frac{1}{r}\frac{\partial}{\partial r}+\frac{\partial^2}{\partial z^2}$$

We define the non-dimensional quantities

$$r'=\frac{\omega}{c_1}r,z'=\frac{\omega}{c_1}z,u_r'=\frac{\omega}{c_1}u_r,u_z'=\frac{\omega}{c_1}u_z,p'=\frac{p}{\lambda},t'=\omega t,\sigma_{zz}'=\frac{\sigma_{zz}}{\lambda},\sigma_{zr}'=\frac{\sigma_{zr}}{\lambda},c_1^2=\frac{\lambda+2\mu}{\rho} \tag{11}$$

where ω is the constant having the dimensions of frequency.

Using dimensionless quantities defined by (11) in Eq. (8)- (10) yield ,

$$\frac{\partial e}{\partial r}+a_1(\nabla^2-\frac{1}{r^2})u_r-a_2\frac{\partial p}{\partial r}=a_3\frac{\partial^2 u_r}{\partial t^2} \tag{12}$$

$$\frac{\partial e}{\partial z}+a_1u_z-a_2\frac{\partial p}{\partial z}=a_3\frac{\partial^2 u_z}{\partial t^2} \tag{13}$$

$$b_1\nabla^2 p-b_2\frac{\partial p}{\partial t}-\frac{\partial e}{\partial t}=0 \tag{14}$$

where

$$a_1=\frac{\mu}{\lambda+\mu}\ ,\ a_2=\frac{\alpha^*\lambda}{\lambda+\mu}\ ,\ a_3=\frac{c_1^2\rho_1}{\lambda+\mu}\ ,\ b_1=\frac{\tau\omega\lambda}{\alpha^* c_1^2}\qquad and\qquad b_2=\frac{\lambda}{\alpha^* M}$$

To simplify the problem, we introduce the potential functions as:

$$u_r=\frac{\partial\Phi}{\partial r}-\frac{\partial\Psi}{\partial z}\ ,\ u_z=\frac{\partial\Phi}{\partial z}+\frac{\partial\Psi}{\partial r}+\frac{\Psi}{r} \tag{15}$$

We define the Laplace and Hankel transforms as follows:

$$\overline{f}(s) = \int_0^\infty f(t)e^{-st}dt \tag{16}$$

$$\tilde{f}(\xi, z, s) = \int_0^\infty \overline{f}(r, z, s) r J_n(r\xi) dr \tag{17}$$

where J_n is the Bessel function of the first kind of index n.

Substituting the values of u_r and u_z from (15) in (12) and (14) and applying the integral transforms defined by (16) and (17) on resulting quantities, we obtain

$$-\xi^2\tilde{\bar{\Phi}} + \frac{d^2\tilde{\bar{\Phi}}}{dz^2} - A_1\tilde{\bar{p}} - B_1\tilde{\bar{\Phi}} = 0 \tag{18}$$

$$-\xi^2\tilde{\bar{\Psi}} + \frac{d^2\tilde{\bar{\Psi}}}{dz^2} - A_2\tilde{\bar{\Psi}} = 0 \tag{19}$$

$$-\xi^2\tilde{\bar{p}} + \frac{d^2\tilde{\bar{p}}}{dz^2} - A_3\xi^2\tilde{\bar{\Phi}} - A_3\frac{d^2\tilde{\bar{\Phi}}}{dz^2} - B_2\tilde{\bar{p}} = 0 \tag{20}$$

Eliminating p from (18) and (20) yields

$$\left[\frac{d^4}{dz^4} - A_{11}\frac{d^2}{dz^2} + B_{11}\right]\tilde{\bar{\Phi}} = 0 \tag{21}$$

where

$$A_{11} = B_1 + B_2 + A_3A_1 + 2\xi^2 \ , \ B_{11} = \xi^4 + (B_1 + B_2 + A_3A_1)\xi^2 + B_1B_2$$

$$\frac{d^4}{dz^4} - A_{11}\frac{d^2}{dz^2} + B_{11} = 0$$

$$\frac{d^2}{dz^2} = \frac{A_{11} \pm \sqrt{{A_{11}}^2 - 4B_{11}}}{2}$$

Solving (21) and (19) and assuming that $\tilde{\bar{\Phi}}, \tilde{\bar{\Psi}}$ and $\tilde{\bar{p}} \to 0$ as $z \to \infty$ we obtain the value of $\tilde{\bar{\Phi}}, \tilde{\bar{\Psi}}$ and $\tilde{\bar{p}}$ as:

$$\tilde{\bar{\Phi}} = C_1e^{-m_1z} + C_2e^{-m_2z} \tag{22}$$

$$\tilde{\bar{\Psi}} = E_1e^{-m_3z} \tag{23}$$

$$\tilde{\bar{p}} = r_1C_1e^{-m_1z} + r_2C_2e^{-m_2z} \tag{24}$$

where m_1, m_2, m_3 are given by $m_n^2 = \frac{A_{11} \pm \sqrt{{A_{11}}^2 - 4B_{11}}}{2}$, (n=1,2), are the roots of the Eq. (21), $m_3 = \sqrt{A_4}$, where $A_4 = A_2 + \xi^2$, and the coupling constants are given by $r_i = \frac{m_i^2 - B_1 - \xi^2}{A_1}$, (i=1,2).

The displacement components $\tilde{\bar{u}}_r$ and $\tilde{\bar{u}}_z$ are obtained with the aid of (15)-(17) and (22)-(24) as:

$$\tilde{\bar{u}}_r = -C_1\xi e^{-m_1z} - C_2\xi e^{-m_2z} + E_1m_3e^{-m_3z} \tag{25}$$

$$\tilde{\tilde{u}}_z = -C_1 m_1 e^{-m_1 z} - C_2 m_2 e^{-m_2 z} + E_1 \xi e^{-m_3 z} \tag{26}$$

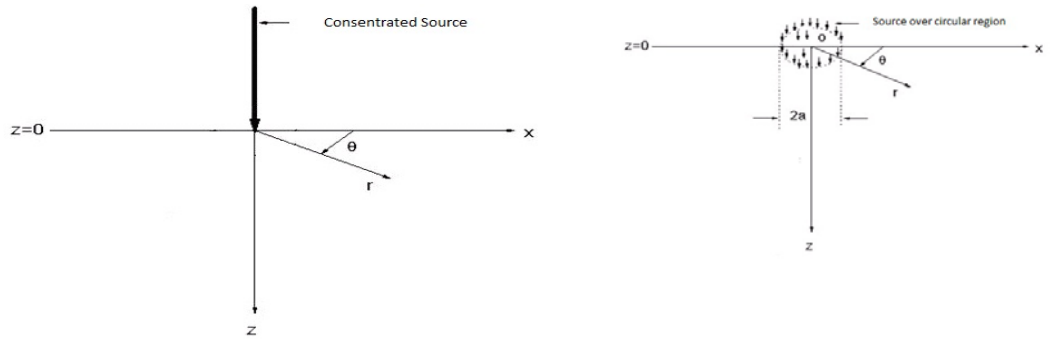

(a) (b)

Fig. 1
(a)Concentrated source acting on the saturated porous media with incompressible fluid half space. (b) Source over the circular region acting on the saturated porous media with incompressible fluid half space.

4 BOUNDARY CONDITIONS AND SOLUTION OF THE PROBLEM

The boundary conditions at z=0 are

$$\sigma_{zz} = -P_1 F(r,t) \ , \ \sigma_{zr} = -P_3 F(r,t) \ , \ p = P_2 F(r,t)$$

where P_1, P_3 are the magnitudes of the forces and P_2 is the constant pressure applied on the boundary and $F(r,t)$ is the known function defined later in the manuscript.

Applying Laplace and Hankel transforms, we have

$$\tilde{\tilde{\sigma}}_{zz} = -P_1 \tilde{\tilde{F}}(\xi,s) \ , \ \tilde{\tilde{\sigma}}_{zr} = -P_3 \tilde{\tilde{F}}(\xi,s) \ , \ \tilde{\tilde{p}} = P_2 \tilde{\tilde{F}}(\xi,s) \tag{27}$$

The stress components are obtained with the aid of (2),(7),(11),(16) and (17) as:

$$\tilde{\tilde{\sigma}}_{zz} = \left[\xi \tilde{\tilde{u}}_r - \alpha \tilde{\tilde{p}} \right] + R_2 \frac{d\tilde{\tilde{u}}_z}{dz} \tag{28}$$

$$\tilde{\tilde{\sigma}}_{zr} = R_1 \left[\frac{d\tilde{\tilde{u}}_r}{dz} - \xi \tilde{\tilde{u}}_z \right] \tag{29}$$

where

$$R_1 = \frac{\mu}{\lambda} \ , \ R_2 = \frac{\lambda + 2\mu}{\lambda}$$

5 DERIVATION OF SECULAR EQUATIONS

Substituting the value of $\tilde{\bar{u}}_r$, $\tilde{\bar{u}}_z$ and $\tilde{\bar{p}}$ from (25),(26) and (24) in the boundary condition (27) and with help of (28) and (29) after some simplifications, we obtain

$$\tilde{\bar{\sigma}}_{zz} = d_1 a_{11} e^{-m_1 z} + d_2 a_{22} e^{-m_2 z} + d_3 a_{33} e^{-m_3 z} \tag{30}$$

$$\tilde{\bar{\sigma}}_{zr} = d_4 a_{11} e^{-m_1 z} + d_5 a_{22} e^{-m_2 z} + d_6 a_{33} e^{-m_3 z} \tag{31}$$

$$\tilde{\bar{p}} = r_1 a_{11} e^{-m_1 z} + r_2 a_{22} e^{-m_2 z} \tag{32}$$

Case 1. For normal force $P_2 = P_3 = 0$

$$\tilde{\bar{\sigma}}_{zz} = d_1 a_{44} e^{-m_1 z} + d_2 a_{55} e^{-m_2 z} + d_3 a_{66} e^{-m_3 z}$$
$$\tilde{\bar{\sigma}}_{zr} = d_4 a_{44} e^{-m_1 z} + d_5 a_{55} e^{-m_2 z} + d_6 a_{66} e^{-m_3 z}$$
$$\tilde{\bar{p}} = r_1 a_{44} e^{-m_1 z} + r_2 a_{55} e^{-m_2 z}$$

Case 2. For tangential force $P_1 = P_2 = 0$

$$\tilde{\bar{\sigma}}_{zz} = d_1 a_{77} e^{-m_1 z} + d_2 a_{88} e^{-m_2 z} + d_3 a_{99} e^{-m_3 z}$$
$$\tilde{\bar{\sigma}}_{zr} = d_4 a_{77} e^{-m_1 z} + d_5 a_{88} e^{-m_2 z} + d_6 a_{99} e^{-m_3 z}$$
$$\tilde{\bar{p}} = r_1 a_{77} e^{-m_1 z} + r_2 a_{88} e^{-m_2 z}$$

Case 3. For pressure force $P_1 = P_3 = 0$

$$\tilde{\bar{\sigma}}_{zz} = d_1 b_{11} e^{-m_1 z} + d_2 b_{22} e^{-m_2 z} + d_3 b_{33} e^{-m_3 z}$$
$$\tilde{\bar{\sigma}}_{zr} = d_4 b_{11} e^{-m_1 z} + d_5 b_{22} e^{-m_2 z} + d_6 b_{33} e^{-m_3 z}$$
$$\tilde{\bar{p}} = r_1 b_{11} e^{-m_1 z} + r_2 b_{22} e^{-m_2 z}$$

where

$$d_1 = -\xi^2 - \alpha r_1 + R_2 m_1^2 \ , \ d_2 = -\xi^2 - \alpha r_2 + R_2 m_2^2 \ , \ d_3 = 2\xi m_3 \ , \ d_4 = 2\xi m_1 R_1 \ , \ d_5 = 2\xi m_2 R_1 \ , \ d_6 = -(m_3^2 + \xi^2) R_1$$

$$a_{11} = \frac{-P_1 \tilde{\bar{F}} r_2 d_6 - P_2 \tilde{\bar{F}} d_2 d_6 + P_2 \tilde{\bar{F}} d_3 d_5 + P_3 \tilde{\bar{F}} r_2 d_3}{\Delta} \ , \ a_{22} = \frac{P_2 \tilde{\bar{F}} d_1 d_6 - P_1 \tilde{\bar{F}} r_1 d_6 - P_3 \tilde{\bar{F}} r_1 d_3 - P_2 \tilde{\bar{F}} d_3 d_4}{\Delta} \ ,$$

$$a_{33} = \frac{-P_3 \tilde{\bar{F}} r_2 d_1 - P_2 \tilde{\bar{F}} d_1 d_5 + P_2 \tilde{\bar{F}} d_2 d_4 + P_3 \tilde{\bar{F}} r_1 d_2 - P_1 \tilde{\bar{F}} r_1 d_5 + P_1 \tilde{\bar{F}} r_2 d_4}{\Delta} \ , \ a_{44} = \frac{-P_1 \tilde{\bar{F}} r_2 d_6}{\Delta} \ , \ a_{55} = \frac{-P_1 \tilde{\bar{F}} r_1 d_6}{\Delta} \ ,$$

$$a_{66} = \frac{-P_1 \tilde{\bar{F}} r_1 d_5 + P_1 \tilde{\bar{F}} r_2 d_4}{\Delta} \ , \ a_{77} = \frac{-P_2 \tilde{\bar{F}} d_2 d_6 + P_2 \tilde{\bar{F}} d_3 d_5}{\Delta} \ , \ a_{88} = \frac{P_2 \tilde{\bar{F}} d_1 d_6 - P_2 \tilde{\bar{F}} d_3 d_4}{\Delta} \ , \ a_{99} = \frac{-P_2 \tilde{\bar{F}} d_1 d_5 + P_2 \tilde{\bar{F}} d_2 d}{\Delta}$$

$$b_{11} = \frac{P_3 \tilde{\bar{F}} r_2 d_3}{\Delta} \ , \ b_{22} = \frac{-P_3 \tilde{\bar{F}} r_1 d_3}{\Delta} \ , \ b_{33} = \frac{-P_3 \tilde{\bar{F}} r_2 d_1 + P_3 \tilde{\bar{F}} r_1 d_2}{\Delta} \ , \ \Delta = r_2 d_1 d_6 - r_1 d_2 d_6 + r_2 d_3 d_5 - r_2 d_3 d_4$$

6 APPLICATION

6.1 Time domain

*Case 1.*Concentrated source:
The solutions due to concentrated source is obtained by substituting

$$F(r,t) = F_1(r)\eta(t) \tag{33}$$

where

$$F_1(r) = \frac{1}{2\pi r}\delta(r) \tag{34}$$

Applying Laplace and Hankel transform on (33) and (34), we obtain

$$\bar{\tilde{F}}(\xi, s) = \frac{1}{2\pi}\bar{\eta}(s)$$

*Case 2.*Source over circular region:
The solution due to source over the circular region of non-dimensional radius a is obtained by setting $F(r,t) = F_1(r)\eta(t)$, where

$$F_1(r) = \frac{1}{\pi a^2}H(a-r)$$

Applying Laplace and Hankel transforms on these quantities, we obtain,

$$\bar{\tilde{F}}(\xi, s) = \frac{1}{\pi a}J_1(a\xi)\bar{\eta}(s)$$

In both the cases, we have taken $\eta(t) = H(t)$, so Laplace transform of $\eta(t)$ gives ,

$$\bar{\eta}(s) = \frac{1}{s}$$

6.2 Frequency domain

In this case, we assume the time harmonic behaviour as:

$$(u_r^i, u_z^i, p)(r,z,t) = (u_r^i, u_z^i, p)(r,z,t)e^{i\omega t}, i = F, S$$

In frequency domain, we take $\eta(t) = e^{i\omega t}$.

The expressions for displacement, stress and pore pressure in frequency domain can be obtained by replacing $i\omega$ in the expressions of time domain (30) - (32) along with $\bar{\eta}(s)$ to be replaced by $e^{i\omega t}$ for concentrated source.

6.3 Special case

In the absence of porous incompressible fluid, the boundary conditions reduce to

$$\tilde{\tilde{\sigma}}_{zz} = -P_1\tilde{\tilde{F}}(\xi, s) \ , \ \tilde{\tilde{\sigma}}_{zr} = -P_3\tilde{\tilde{F}}(\xi, s)$$

and we obtain the constituting expressions for stress components in elastic half space as:

$$\tilde{\tilde{\sigma}}_{zz} = d_7 b_{44} e^{-m_4 z} + d_8 b_{55} e^{-m_3 z} \tag{35}$$

$$\tilde{\tilde{\sigma}}_{zr} = d_9 b_{44} e^{-m_4 z} + d_6 b_{55} e^{-m_3 z} \tag{36}$$

where,

$$d_7 = -\xi^2 + R_2 m_4^2 \ , \ d_8 = (1 - R_2)\xi m_3 \ , \ d_9 = 2\xi m_4 R_1 \ ,$$

$$b_{44} = \frac{-P_1\tilde{\tilde{F}}d_6 + P_3\tilde{\tilde{F}}d_8}{\Delta_{10}} \ , \ b_{55} = \frac{-P_3\tilde{\tilde{F}}d_7 + P_1\tilde{\tilde{F}}d_9}{\Delta_{10}} \ , \ \Delta_{10} = d_6 d_7 - d_8 d_9$$

Taking $P_3 = 0$ and $P_1 = 0$ in Eqs. (35) and (36), we obtain respectively the stress components for the normal and tangential forces.

7 NUMERICAL RESULTS AND DISCUSSION

With the view of illustrating the theoretical results and for numerical discussion we take a model for which the value of the various physical parameters are taken from Gatmiri and Ngyun[6]:

$$\lambda = 12.5MPa \ , \ \mu = 8.33MPa \ , \ K_s = 10^5 MPa \ , \ K_f = 0.22 \times 10^4 MPa \ , \ \rho_s = 2600Kg/m^3 \ ,$$
$$\rho_f = 1000Kg/m^3 \ , \ k = 0.001m/s \ , \ \alpha = 1 \ , \ n = 0.3 \ , \ \omega = 1$$

The values of normal stress σ_{zz}, tangential stress σ_{zr} and pore pressure p for fluid saturated incompressible porous medium (FSPM) and empty porous medium (EPM) are shown due to concentrated source and source applied over the circular region.The computation are carried out for two values of dimensionless time *t*=0.1 and *t*=0.5 at *z*=1 in the range $0 \le r \le 10$.

The solid lines either without central symbols or with central symbols represents the variations for t=0.1, whereas the dashed lines with or without central symbols represents the variations for *t*=0.5.Curves without central symbols correspond to the case of FSPM whereas those with central symbols corresponds to the case of EPM.

7.1 Time domain

Fig.2 shows the variation of normal stress component σ_{zz} w.r.t distance *r* for both FSPM and EPM due to concentrated normal force. The value of σ_{zz} starts with initial increase and then oscillates for FSPM as *r* increases and in case of EPM, its value oscillates as *r* increases for both values of time. Fig. 3 shows the variation of normal stress component σ_{zz} w.r.t distance *r* for both FSPM and EPM due to concentrated tangential force. The value of σ_{zz} oscillates for FSPM as *r* increases for both values of time whereas in case of EPM , the value of σ_{zz} starts with sharp decrease and then oscillates for both values of time as *r* increases. Fig. 4 shows the variation of normal stress component σ_{zz} w.r.t distance *r* for FSPM due to concentrated pressure source. The value of σ_{zz} is more in the range $3 \le r \le 6$ and less in the range $6 \le r \le 9$ for FSPM as *r* increases for time *t*=0.1 whereas for the time *t*=0.5 its value converges near the boundary surface.

Fig. 5 shows the variation of pore pressure *p* w.r.t distance *r* for FSPM due to concentrated normal force. The value of *p* starts with initial decrease and then oscillates for FSPM as *r* increases for time *t*=0.1 whereas for the time *t*=0.5 the value of *p* decreases sharply and then oscillates as *r* increases.

Fig. 6 shows the variation of pore pressure p w.r.t distance r for FSPM due to concentrated tangential force. The value of p converges near the boundary surface for FSPM as r increases for time t=0.1 whereas for the time t=0.5 the value of p decreases sharply and then oscillates as r increases. Fig.7 shows the variation of pore pressure p w.r.t distance r for FSPM due to concentrated pressure source. The value of p converges near the boundary surface for FSPM as r increases for time t=0.1 whereas for the time t=0.5 the value of p increases sharply and then oscillates as r increases. Fig.8 shows the variation of tangential stress σ_{zr} w.r.t distance r for both FSPM and EPM due to concentrated normal force. The value of σ_{zr} first decreases and then oscillates for FSPM as r increases for both value of time where as the value of σ_{zr} decreases sharply and then oscillates for EPM as r increases for both value of time. Fig.9 shows the variation of tangential stress σ_{zr} w.r.t distance r for both FSPM and EPM due to concentrated tangential force. The value of σ_{zr} first increases monotonically and then converges near the boundary surface for FSPM and EPM as r increases for both value of time.

Fig.10 shows the variation of tangential stress σ_{zr} w.r.t distance r for FSPM due to concentrated pressure source. The value of σ_{zr} first increases and then oscillates for FSPM as r increases for time t=0.1 where as for the time t=0.5 the value of σ_{zr} starts with initial increase and then converges near the boundary surface. Fig.11 shows the variation of normal stress σ_{zz} w.r.t distance r for both FSPM and EPM due to normal force over circular region. The value of σ_{zz} starts with initial increase and then oscillates for FSPM and EPM as r increases for both value time.

Fig.12 shows the variation of normal stress σ_{zz} w.r.t distance r for both FSPM and EPM due to tangential force over circular region. The value of σ_{zz} starts oscillates for FSPM as r increases for both value time and the value of σ_{zz} for EPM first decreases gradually and then starts oscillating as r increases for both value time. Fig.13 shows the variation of normal stress σ_{zz} w.r.t distance r for FSPM due to pressure source over circular region. The value of σ_{zz} first increases monotonically and then oscillates for FSPM as r increases for time t=0.1 where as for the time t=0.5 the value of σ_{zz} converges near the boundary surface as r increases.

Fig. 14 shows the variation of pore pressure p w.r.t distance r for FSPM due to normal force over circular region. The value of p decreases sharply and then oscillates as r increases for both value of time. Fig.15 shows the variation of pore pressure p w.r.t distance r for FSPM due to tangential force over circular region. The value of p converges near the boundary surface for FSPM as r increases for time t=0.1 whereas for the time t=0.5 the value of p decreases sharply and then oscillates as r increases. Fig.16 shows the variation of pore pressure p w.r.t distance r for FSPM due to pressure source over circular region. The value of p starts with initial increase and then oscillates for FSPM as r increases for time t=0.1 where as for the time t=0.5 the value of p increases sharply in the range $0 \le r \le 5$ and then starts decreasing as r increases. Fig. 17 shows the variation of tangential stress σ_{zr} w.r.t distance r for both FSPM and EPM due to normal force over circular region. The value of σ_{zr} first decreases and then oscillates for FSPM as r increases for both value of time where as the value of σ_{zr} decreases gradually and then oscillates for EPM as r increases for both value of time.

Fig.18 shows the variation of tangential stress σ_{zr} w.r.t distance r for both FSPM and EPM due to tangential force over circular region. The value of σ_{zr} first increases monotonically and then converges near the boundary surface for FSPM for both value of time where as the value of σ_{zr} converges near the boundary surface for time t=0.1 and first increases monotonically and then converges near the boundary surface for the time t=0.5 for EPM as r increases. Fig.19 shows the variation of tangential stress σ_{zr} w.r.t distance r for FSPM due to pressure source over circular region. The value of σ_{zr} increases sharply and then oscillates as r increases for FSPM for both value of time.

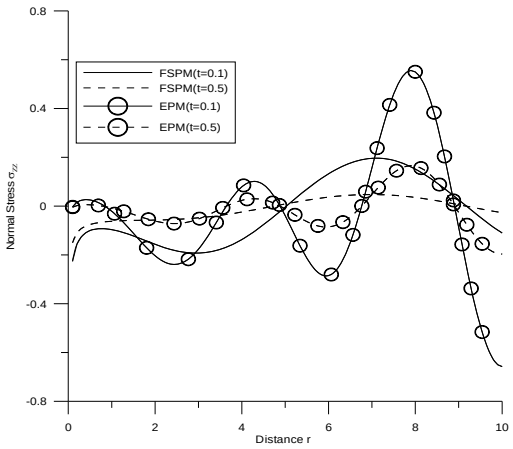

Fig. 2
Variation of normal stress σ_{zz} with distance *r* due to concentrated Normal force.

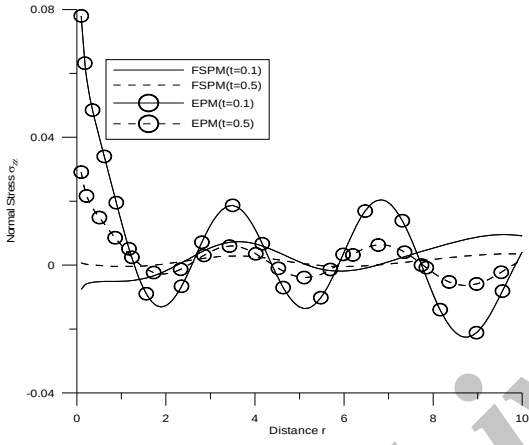

Fig. 3
Variation of normal stress σ_{zz} with distance *r* due to concentrated tangential force.

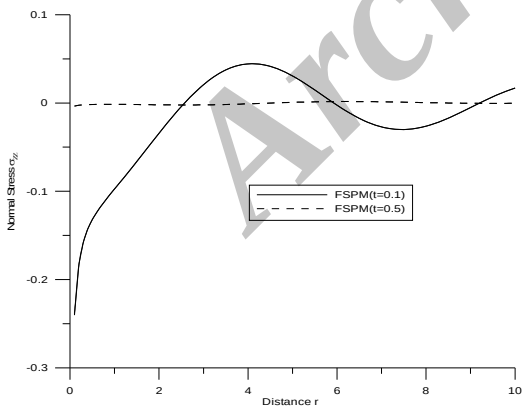

Fig. 4
Variation of normal stress σ_{zz} with distance *r* due to concentrated pressure source.

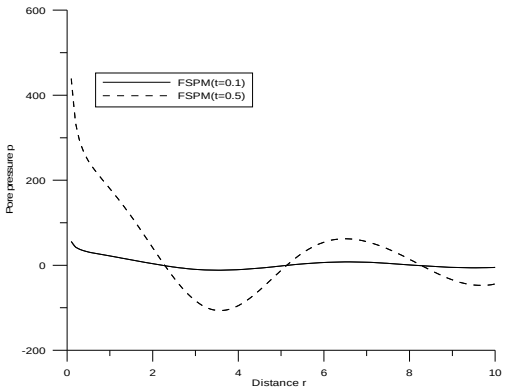

Fig. 5
Variation of pore pressure p with distance r due to concentrated normal force.

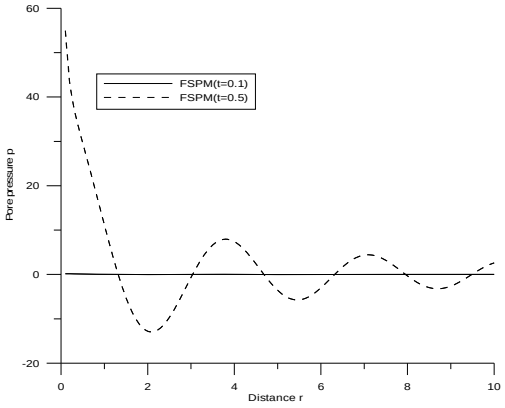

Fig. 6
Variation of pore pressure p with distance r due to concentrated tangential force.

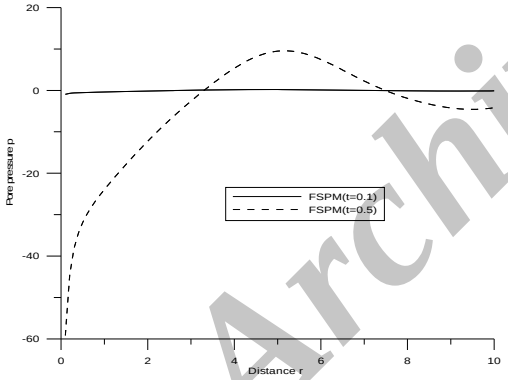

Fig. 7
Variation of pore pressure p with distance r due to concentrated pressure source.

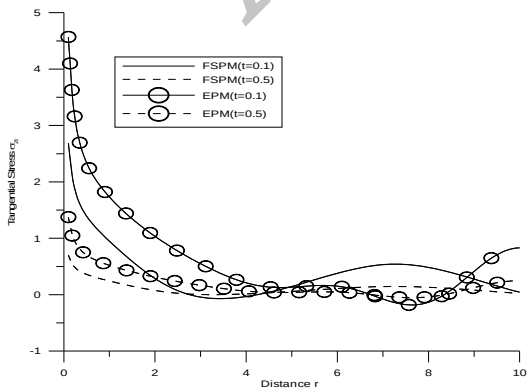

Fig. 8
Variation of tangential stress σ_{Zr} with distance r due to concentrated Normal force.

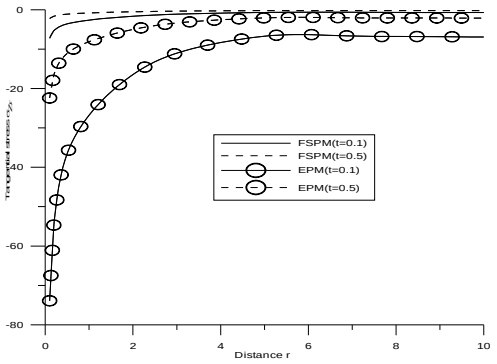

Fig. 9
Variation of tangential stress σ_{Zr} with distance *r* due to concentrated tangential force**.**

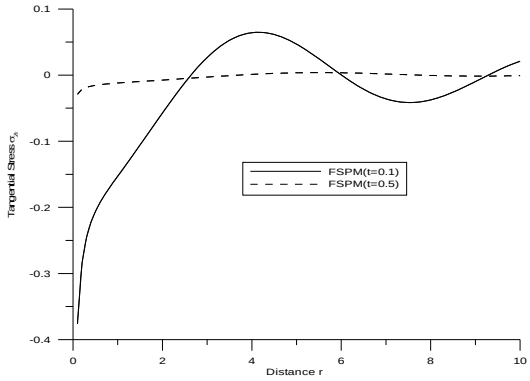

Fig. 10
Variation of tangential stress σ_{Zr} with distance *r* due to concentrated pressure source.

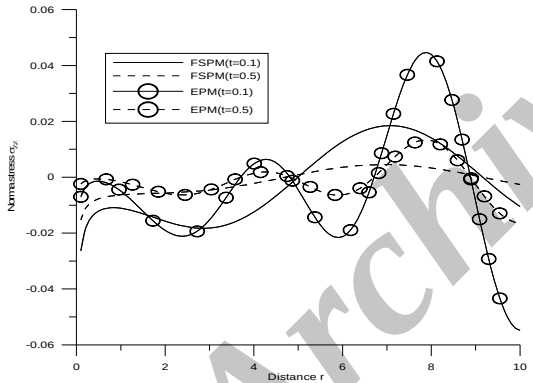

Fig. 11
Variation of normal stress σ_{ZZ} with distance *r* due to normal force over circular region.

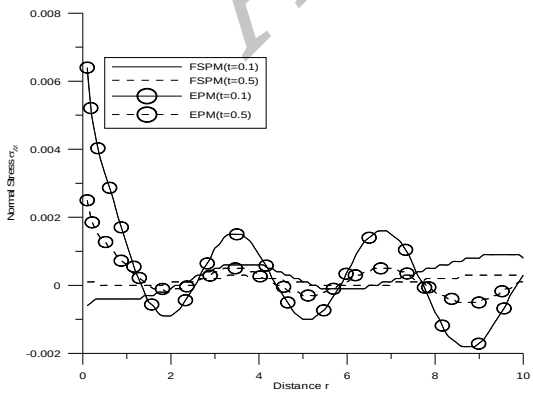

Fig. 12
Variation of normal stress σ_{ZZ} with distance *r* due to tangential force over circular region.

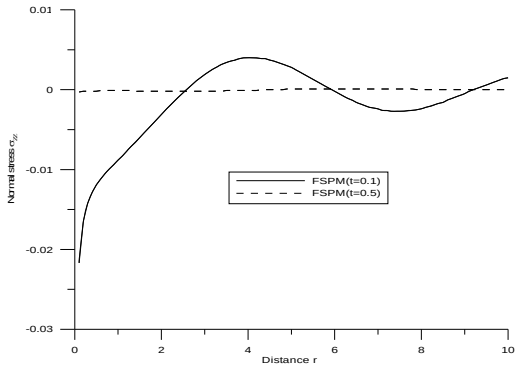

Fig. 13
Variation of normal stress σ_{ZZ} with distance *r* due to normal force over circular region.

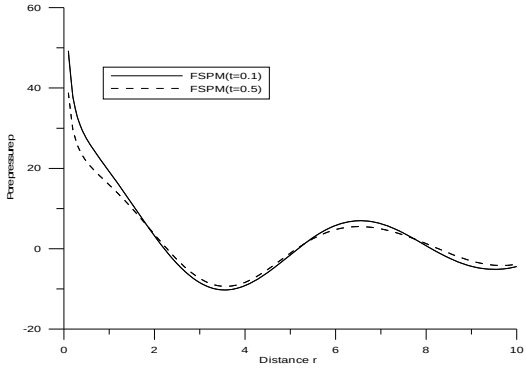

Fig. 14
Variation of pore pressure *p* with distance *r* due to normal force over circular region.

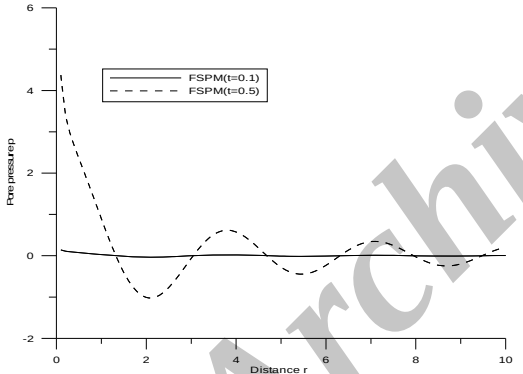

Fig. 15
Variation of pore pressure *p* with distance *r* due to tangential force over circular region.

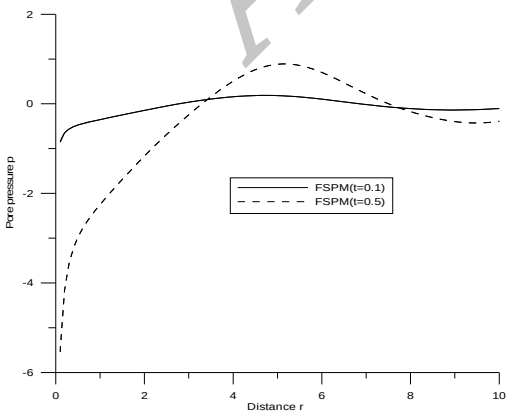

Fig. 16
Variation of pore pressure *p* with distance *r* due to pressure source over circular region.

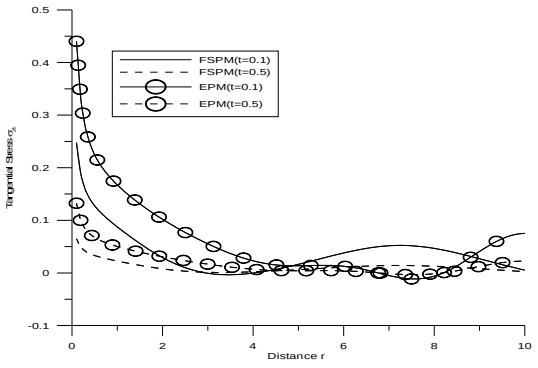

Fig. 17
Variation of tangential stress σ_{Zr} with distance *r* due to normal force over circular region.

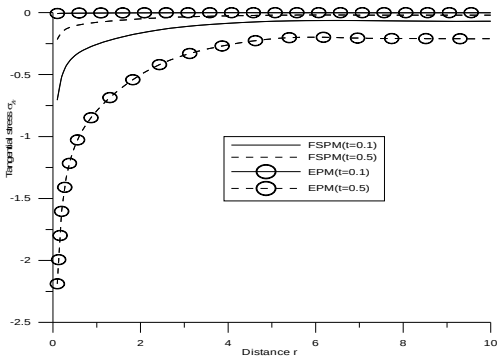

Fig. 18
Variation of tangential stress σ_{Zr} with distance *r* due to normal force over circular region.

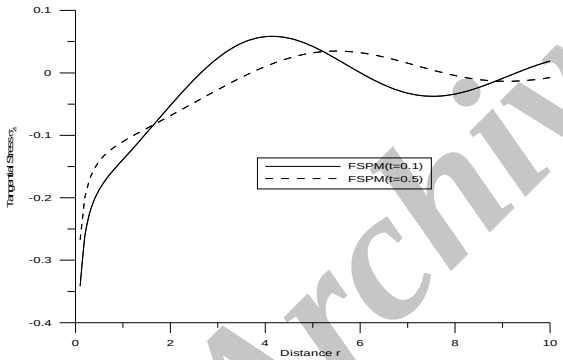

Fig. 19
Variation of tangential stress σ_{Zr} with distance *r* due to pressure source over circular region.

7.2 Frequency domain

Fig. 20 shows the variation of normal stress component σ_{zz} w.r.t distance *r* for both FSPM and EPM due to concentrated normal force. The value of σ_{zz} first increases monotonically and then start oscillating for FSPM as *r* increases for both value the time where as its value oscillates as *r* increases for *t*=0.1 and converges near the boundary surface for *t*=0.5 for EPM. Fig.21 shows the variation of normal stress component σ_{zz} w.r.t distance *r* for both FSPM and EPM due to concentrated tangential force. The value of σ_{zz} first decreases sharply and then start oscillating for FSPM as *r* increases for both value the time where as its value oscillates as *r* increases for both value the time for EPM.

Fig. 22 shows the variation of normal stress component σ_{zz} w.r.t distance *r* for FSPM due to concentrated pressure source. The value of σ_{zz} first decreases and then start oscillates for FSPM as *r* increases for both value of time. Fig. 23 shows the variation of pore pressure *p* w.r.t distance *r* for FSPM due to concentrated normal source. The value of *p* first increases sharply and then start oscillates for FSPM as *r* increases for both value of time.

Fig. 24 shows the variation of pore pressure p w.r.t distance r for FSPM due to concentrated tangential source. The value of p decreases and then start oscillates for FSPM as r increases for both value of time. Fig. 25 shows the variation of pore pressure p w.r.t distance r for FSPM due to concentrated pressure source. Fig. 26 shows the variation of tangential stress σ_{zr} w.r.t distance r for both FSPM and EPM due to concentrated normal force. The value of σ_{zr} first increases sharply and then start oscillates for time t=0.1 where as for the time t=0.5 the value of σ_{zr} first increases and then converges near the boundary surface as r increases for FSPM and for EPM it value first increases monotonically and then start oscillates for time t=0.1 where as for the time t=0.5 the value of σ_{zr} converges near the boundary surface as r increases. Fig. 27 shows the variation of tangential stress σ_{zr} w.r.t distance r for both FSPM and EPM due to concentrated tangential source. The value of σ_{zr} decreases gradually for time t=0.1 where as for the time t=0.5 the value of σ_{zr} first increases and then converges near the boundary surface as r increases for FSPM and for EPM it value first decreases monotonically and then start oscillates for time t=0.1 where as for the time t=0.5 the value of σ_{zr} converges near the boundary surface as r increases.

Fig. 28 shows the variation of tangential stress σ_{zr} w.r.t distance r for FSPM due to concentrated pressure source. The value of σ_{zr} decreases gradually and then start oscillates for time t=0.1 where as for the time t=0.5 the value of σ_{zr} first decreases and then converges near the boundary surface for FSPM as r increases.

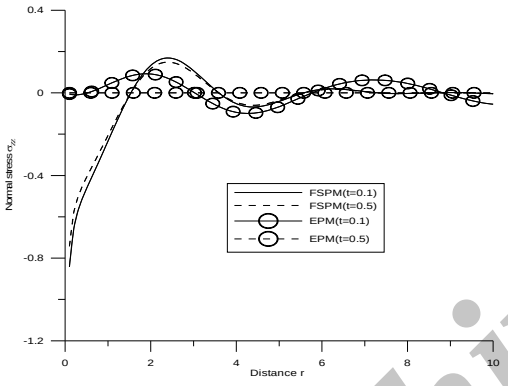

Fig. 20
Variation of normal stress σ_{ZZ} with distance r due to normal force (frequency domain).

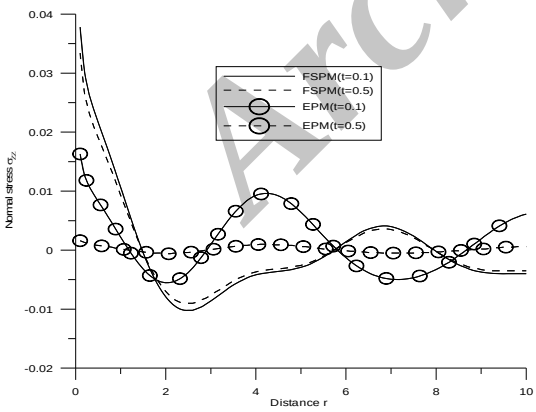

Fig. 21
Variation of normal stress σ_{ZZ} with distance r due to tangential source (frequency domain).

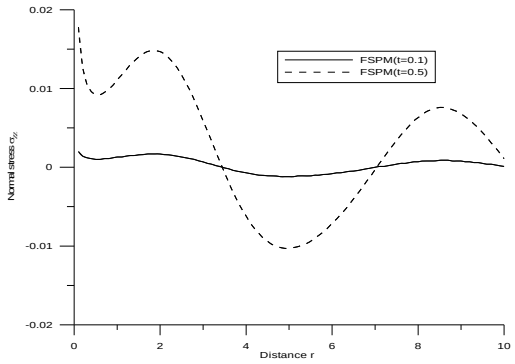

Fig. 22
Variation of normal stress σ_{ZZ} with distance *r* due to pressure source (frequency domain).

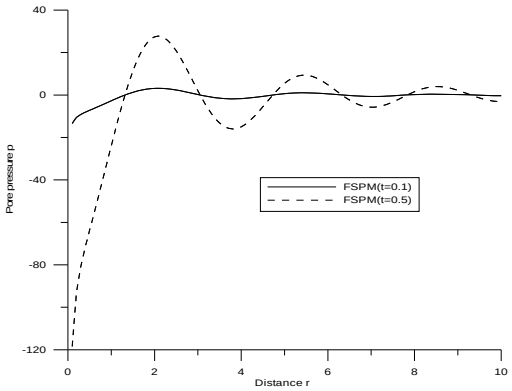

Fig. 23
Variation of pore pressure *p* with distance *r* due to normal force (frequency domain).

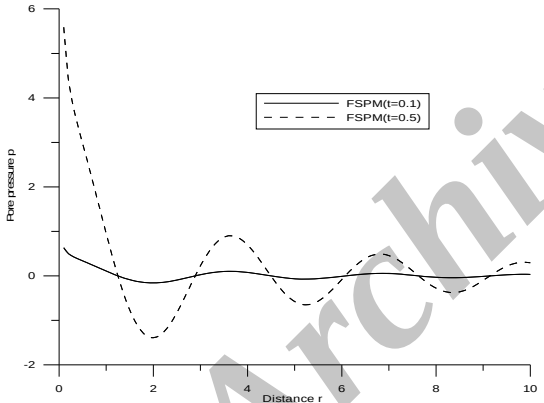

Fig. 24
Variation of pore pressure *p* with distance *r* due to tangential force (frequency domain).

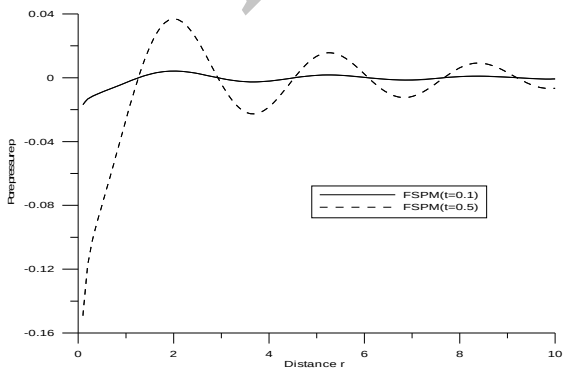

Fig. 25
Variation of pore pressure *p* with distance *r* due to pressure source (frequency domain).

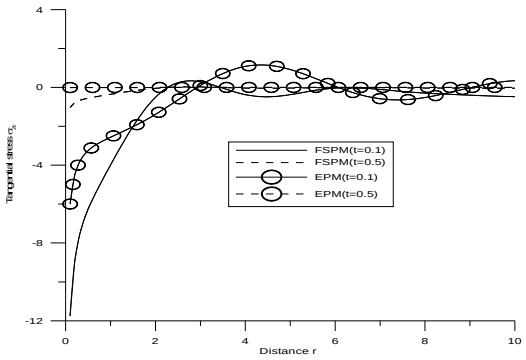

Fig. 26
Variation of tangential stress σ_{Zr} with distance *r* due to normal force (frequency domain).

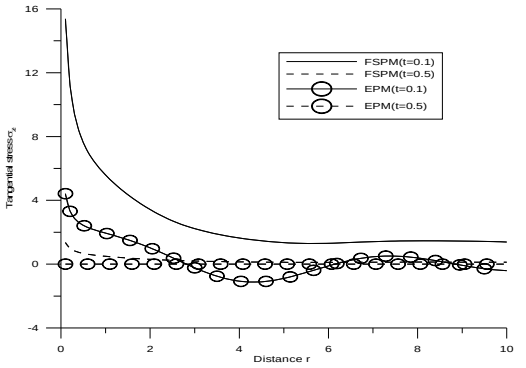

Fig. 27
Variation of tangential stress σ_{Zr} with distance *r* due to tangential force (frequency domain).

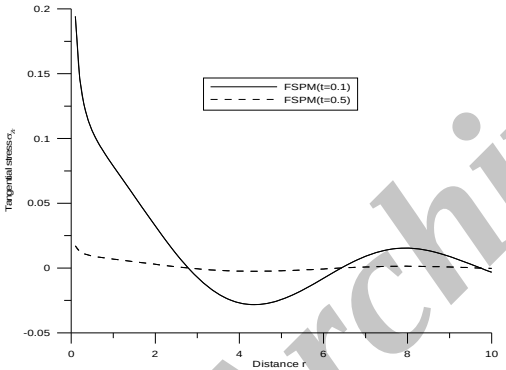

Fig. 28
Variation of tangential stress σ_{Zr} with distance *r* due to pressure source (frequency domain).

8 CONCLUSIONS

Near the application of the source, the porosity effect decreases the values of σ_{zz} for normal force, tangential force and pressure source where as it decreases the values of σ_{zr} for normal force and tangential force but increase the values for pressure source, due to concentrated source in the time domain. In frequency domain, porosity effect increases the values of σ_{zz} and σ_{zr} and *p* for normal force, tangential force and pressure source for source over circular region. Also away from the source, the porosity effect decreases the values of σ_{zz} for normal force and increases the values for tangential force and pressure source whereas it decreases the value of σ_{zr} for normal force and monotonically increases for tangential force and pressure source. In the intermediate region, the values of σ_{zz} σ_{zr} and *p* oscillates for all the sources in both the domains.

REFERENCES

[1] Biot MA., 1956, Theory of propagation of elastic waves in fluid saturated porous solid I-low frequency range, *Journal of the Acoustical Society of America* **28**:168-178.

[2] Prevost JH.,1980, Mechanics of continuous porous media, *International journal of Engineering Science* **18**:787-800.

[3] Zenkiewicz OC., Chang CT., Bettess P., Drained., 1980, Consolidating and dynamic behavior assumptions in soils, *Geotechnique* **30**(4):385-395.

[4] Zenkiewicz OC., Shiomi T., 1984, Dynamic behavior of saturated porous media: the generalized Biot formulation and its numerical solution, *International Journal of Numerical and Analytical methods in Geomechanics* **8**: 71-96.

[5] Gatmiri B., Kamalian M., 2002, On the fundamental solution of dynamic poroelastic boundary integral equations in the time domain, *The International Journal of Geomechanics* **2**(4): 381-398.

[6] Gatmiri B., Nguyen KV., 2005, Time 2D fundamental solution for saturated porous media with incompressible fluid, *Communications in Numerical Methods in Engineering* **21**:119-132.

[7] Gatmiri B., Jabbari M., 2005, Time domain Green's functions for unsaturated soil, *International Journal of Solid and Structure* **42**:5971-5990.

[8] Gatmiri B., Jabbari M., 2005, Time domain Green's functions for unsaturated soil, *International Journal of Solid and Structure* **42**:5991-6002.

[9] Gatmiri B., Maghoul P., Duhamel D., 2010, Two-dimensional transient thermo-hydro-mechanical solutions of multiphase porous media in frequency and time domain, *International Journal of Solid and Structure* **47**:595-610.

[10] Gatmiri B., Eslami H., 2007, The scattering of harmonic waves by a circular cavity in a porous medium: complex function theory approach, *International Journal of Geomechanics* **7**(5): 371-381.

[11] Kumar R., Singh R., Chadha TK., 2002, Axisymmetric problem in microstrectch elastic solid, *Indian Journal of Mathematics* **44**:147-164.

[12] Kumar R., Singh R., 2005, Elastodynamics of an axisymmetric problem in microstrectch visco elastic solid, *International Journal of Applied Mechanics and Engineering* **10**:227-244.

[13] Kaushal S., Kumar R., Miglani A., 2010, Response of frequency domain in generalized thermoelasticity with two temperature, *Journal of Engineering Physics and Thermophysics* **83**(5): 1080-1088.

[14] Kumar R., Garg NR., Miglani A., 2003, Elastodynamics of an axisymmetric problem in an anisotropic liquid-saturated porous medium, *Journal of Sound and Vibration* **261**:697-714.

[15] Oliveira MMF., Dumont NA., Selvadura APS., 2012, Boundary element formulation of axisymmetric problems for an elastic halfspace, *Engineering Analysis with Boundary Elements*, **36**(10):1478-1492.

[16] Akbarob SD., Guliev MS., 2010, The influence of the finite initial strain on the axisymmetirc wave dispersion in a circular cylinder embedded in a compressible elastic medium,*International Journal of Mechanical Sciences*, **52**(1): 89-95.

[17] Gordeliy E., Detourna E., 2011, Displacement discontinuity method for modeling axisymmetric cracks in an elastic half-space, *International Journal of Solids and Structures*, **48**(19):2614-2629.